



A Flank Correction Methodology for Hob Sharpening on the Five-Axis CNC Hob Sharpening Machine

Yi-Pei Shih¹ and Shi-Duang Chen²

¹National Taiwan University of Science and Technology, shihyipei@mail.ntust.edu.tw

²Luren Precision Co., Ltd., chuck_chen@luren.com.tw

ABSTRACT

Hobbing is the most widely employed cutting method for producing cylindrical gears, splines, and so on. However, because the wearing of the hob cutters always reduces their accuracy, the tooth faces on the hob gashes must be reground to ensure the accuracy of the machined gear and prolong the cutter's lifetime. In practice, the deviations of the ground tooth face of hob gashes are caused by machine error. This paper thus proposes a high-order flank correction method based on the degrees of freedom in the five-axis computer numerical control (CNC) hob sharpening machine. The behavior of each axle of the grinding machine is described by high-order polynomials, and the sensitivity of the polynomial coefficient is derived based on the topographic normal deviation on the tooth face. The ground tooth face can then be approximated to the theoretical tooth face by adjusting the coefficients of the polynomials based on their sensitivity. We demonstrate the validity of this flank correction method numerically using a helical gash hob ground by the five-axis CNC hob sharpening machine.

Keywords: hob sharpening, flank correction methodology, five-axis CNC.

DOI: 10.3722/cadaps.2012.585-598

1 INTRODUCTION

Progressive cutting into gear teeth by a cutting tool using the generating method is called hobbing. Because it is efficient, accurate, and inexpensive, hobbing has become the most widely employed cutting process for such products as cylindrical gears and splines. Once the hob cutter has become worn, however, the tooth faces on the hob gashes must be reground to maintain the correct profile of the cutting edges. Such tool resharpener reduces cutter breakage and guarantees the precision of the workpiece profile. There are two types of gash - a straight gash, which must be parallel with the hob axle, and a helical gash, which should be normal to the thread helix. In theory, all hobs should have

helical gashes to ensure an even cutting force on both sides of the tooth during the hobbing process. In practice, however, because of manufacturing considerations, the straight gash is allowed in small thread angles to simplify hob design and manufacture, while the helical gash is widely adopted in large thread angles like worm gear hobs for a better cutting condition. The sharpening machine generally includes at least four axes to satisfy the demand of degrees of freedom for grinding.

The newly developed hob sharpening machines, such as the Klingelnberg S31-series and the Luren Precision LGH-series, are all Cartesian-type structures with five movable axes controlled by computer numerical control (CNC). Because of state-of-the-art CNC technology, these machines can offer a precise simultaneous four-axis movement that enables an accurate tooth face on the gashes. All are designed to grind the tooth faces of both straight- and helical-gash hobs using the form grinding method. However, because of the inevitable machine errors, the ground tooth face is not perfect. Therefore, the existing on-machine manufacturing software provides simple correction functions to reduce surface deviations. The corrective result, however, is highly dependent on the machine operator's skill and experience.

The form grinding process, of which hob sharpening is a type, has been widely studied. For example, Yoshino et al. [1] proposed a flank correction method for form grinding through compensation of the wheel profile and the position between the wheel and the work gear. Subsequently, in extensive research, Nishida et al. derived the wheel profile using an analytical method [2], proposed an optimum contact-line shape by modulating the setting angle of the wheel for tooth trace modification [3], and then estimated the accuracy of the gear tooth profile corresponding to the wheel setting errors [4]. Litvin et al. [7] discussed the form grinding method for involute helicoids and interpreted the corresponding core theory. For the manufacture of hob gashes, Chang proposed a mathematical model for the hob gash tooth face and, after investigating a disk- and pencil- type grinding wheel for hob sharpening [5], developed a mathematical model of hob gashes produced by milling cutters [6]. More recently, Shih et al. [8] proposed flank correction methodology based on the six-axis Cartesian-type CNC hypoid generator. Their method for spiral bevel and hypoid gears provide a foundation for our development of a flank correction methodology for sharpening the tooth faces of hob gashes.

This research aims to establish a free-form flank correction methodology based on the five-axis CNC hob sharpening machine. Specifically, we propose a mathematical model of the five-axis machine to meet the needs of the modern CNC hob sharpening machine. The five-axis movement correction is derived using the measured topographic errors of the tooth face and a sensitivity analysis of the proposed mathematical model. This paper clearly illustrates the feasibility of the proposed flank correction method using a numerical example of a helical-gash hob ground by the proposed five-axis machine, which is comparable to the Klingelnberg S31-series and the Luren Precision LGH-series hob sharpening machines.

2 MATHEMATICAL MODEL OF THE WHEEL AXIAL PROFILE

Hob sharpening is a form grinding process that is implemented in both straight and helical gashes. The tooth face of the hob gash is ground using a disk-type wheel whose axial profile is a straight line for straight-gash grinding but a convex curve for helical-gash grinding. The hob sharpening (form grinding) process is highly productive because of the line contact between the grinding wheel and the tooth face of the hob gash. However, as widely recognized, the axial profiles of the wheel depend on the ground tooth face, the center distance between the wheel and the hob, and the setting angle of the wheel. The wheel profile must therefore be determined before the grinding process. In prior research, the mathematical model of the wheel surface has been derived from a universal machine, so in this

proposed correction method, the machine settings of the CNC machine are still translated from the universal machine. For clarity, the previous mathematical models are rewritten in this section.

As shown in Fig. 1, the tooth face of a hob gash is a helicoid generated by a straight line. The rake angle γ_c is an angle of inclination of the tooth face from the reference plane R and may be positive, negative, or even zero depending on the material machined. In practice, a zero-rake angle is frequently used to simplify hob design and manufacture.

In determining the wheel's axial profile, the hob's ground tooth face, a helicoid generated by a straight line, is considered a given. The straight line is represented in coordinate system S_q by

$$\mathbf{r}_q(u) = \{0 \quad r_p \cos \gamma_c + u \quad e \quad 1\}^T, \quad \gamma_c = \sin^{-1}\left(\frac{e}{r_p}\right), \quad (1)$$

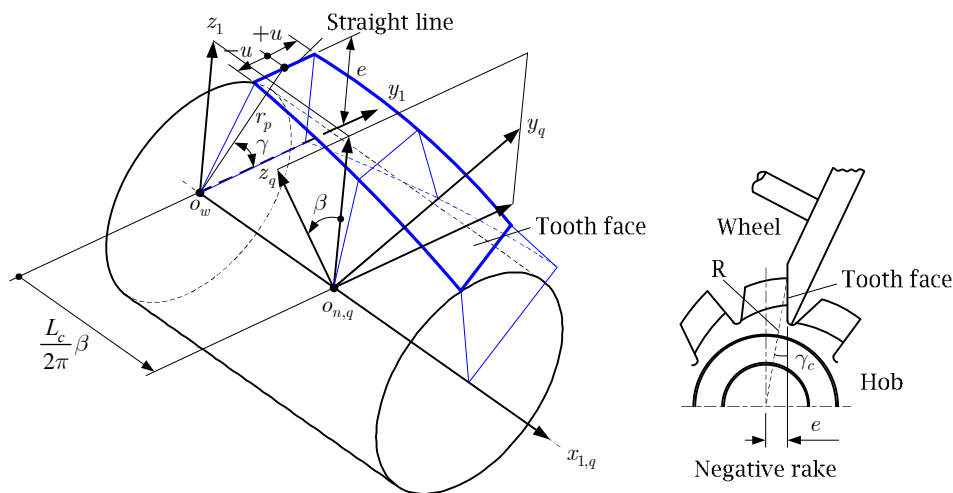


Fig. 1: Coordinate systems of the tooth face on the hob gash (right hand).

where u is the independent variable of the straight line, r_p is the pitch radius of the hob, and e is the rake offset. According to the lead L_c of the gash, the helicoid is determined in coordinate system S_1 with the matrix equation

$$\mathbf{r}_1(u, \beta) = \mathbf{M}_{1q}(\beta) \mathbf{r}_q(u) \quad (2)$$

where

$$\mathbf{M}_{1q}(\beta) = \begin{bmatrix} 1 & 0 & 0 & \frac{L_c}{2\pi} \beta \\ 0 & \cos \beta & -\sin \beta & 0 \\ 0 & \sin \beta & \cos \beta & 0 \\ 0 & 0 & 0 & 1 \end{bmatrix}$$

Based on the theory of conjugate surfaces, the contact lines on the tooth face and wheel construct their respective surfaces; hence, using a tooth face as a virtual tool for inversely grinding the wheel allows derivation of the wheel axial profile. This spatial relationship between the wheel and the ground

tooth face in the universal hob sharpening machine is shown in Fig. 2. Such a virtual machine has three universal machine settings, E_t , γ_m , and L_t , the center distance between the wheel and hob centers, the setting angle of the wheel, and the axial movement along the hob axis, respectively. In standard operation, the first two terms are constant and the last is a linear function of the hob's rotation angle. Although in general, the setting angle of the wheel γ_m is equal to the helical angle of the gash, occasionally that angle is adjusted slightly to control the shape of the contact line, thereby improving the grinding condition [3].

The transformation matrices S_1 to S_t give the surface locus of the given tooth face in coordinate system S_t :

$$\mathbf{r}_t(u, \beta, \phi_1) = \{x_t \ y_t \ z_t \ 1\}^T = \mathbf{M}_{tc}(\eta)\mathbf{M}_{cb}(\gamma_m)\mathbf{M}_{ba}(E_t, L_t)\mathbf{M}_{a1}(\phi_1)\mathbf{r}_1(u, \beta) = \mathbf{M}_{t1}(\eta, \gamma_m, E_t, L_t, \phi_1)\mathbf{r}_1(u, \beta) \quad (3)$$

Here,

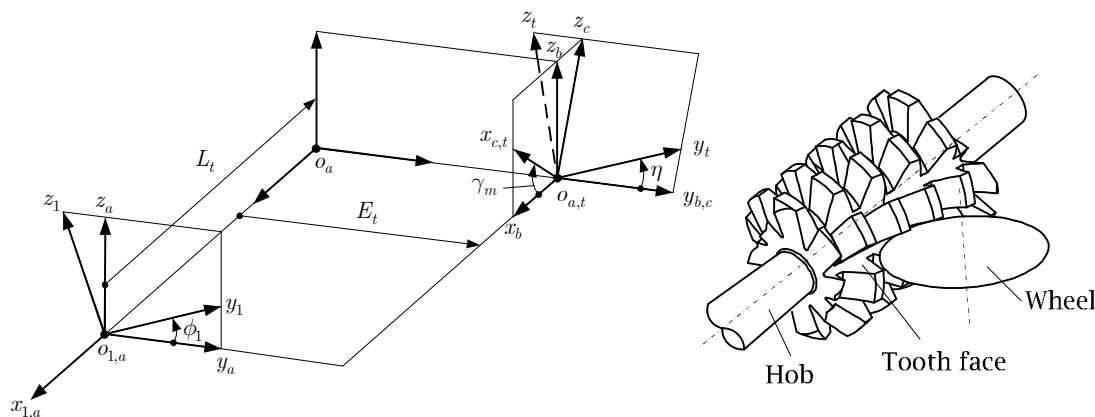


Fig. 2: Coordinate systems of a universal hob sharpening machine.

$$\mathbf{M}_{tc}(\eta) = \begin{bmatrix} 1 & 0 & 0 & 0 \\ 0 & \cos \eta & \sin \eta & 0 \\ 0 & -\sin \eta & \cos \eta & 0 \\ 0 & 0 & 0 & 1 \end{bmatrix}, \quad \mathbf{M}_{cb}(\gamma_m) = \begin{bmatrix} \cos \gamma_w & 0 & \sin \gamma_w & 0 \\ 0 & 1 & 0 & 0 \\ -\sin \gamma_w & 0 & \cos \gamma_w & 0 \\ 0 & 0 & 0 & 1 \end{bmatrix},$$

$$\mathbf{M}_{ba}(E_t, L_t) = \begin{bmatrix} 1 & 0 & 0 & L_t \\ 0 & 1 & 0 & -E_t \\ 0 & 0 & 1 & 0 \\ 0 & 0 & 0 & 1 \end{bmatrix}, \quad \text{and } \mathbf{M}_{a1}(\phi_1) = \begin{bmatrix} 1 & 0 & 0 & 0 \\ 0 & \cos \phi_1 & -\sin \phi_1 & 0 \\ 0 & \sin \phi_1 & \cos \phi_1 & 0 \\ 0 & 0 & 0 & 1 \end{bmatrix}.$$

where the parameters L_t and the work-piece rotation angle ϕ_1 are usually related as $L_t = P_t \phi_1$, and P_t is the screw parameter, which is determined based on the helical angle of the hob's pitch cylinder. During the grinding process, the universal machine settings are constants or a linear function. According to differential geometry, if the work-piece rotation angle ϕ_1 is the motion parameter, the locus normal can be derived as follows:

$$\mathbf{n}_t(u, \beta, \phi_1) = \frac{\frac{\partial \mathbf{r}_t(u, \beta, \phi_1)}{\partial u} \times \frac{\partial \mathbf{r}_t(u, \beta, \phi_1)}{\partial \beta}}{\left| \frac{\partial \mathbf{r}_t(u, \beta, \phi_1)}{\partial u} \times \frac{\partial \mathbf{r}_t(u, \beta, \phi_1)}{\partial \beta} \right|} \quad (4)$$

As illustrated in Fig. 3, when the wheel surface is conjugated to the tooth face, the normal \mathbf{n}_t on the contact line between the two surfaces must pass through the wheel axis \mathbf{z}_t . Because the three vectors \mathbf{n}_t , \mathbf{z}_t and \mathbf{r}_t are coplanar, then according to the equation of meshing, the scalar triple product is equal to zero, as shown by the following equation:

$$f_t = \mathbf{n}_t(u, \beta, \phi_1) \cdot [\mathbf{z}_t \times \mathbf{r}_t(u, \beta, \phi_1)] = 0 \quad (5)$$

Solving the contact line in coordinate system S_t allows determination of the wheel profile. Because in the form grinding process the contact lines are identical at every instant - that is, the rotation angle of the work-piece is $\phi_1 = 0$ - the contact points can be solved using Eqn. (5) plus one boundary equation of the wheel. Equation (6) can then be used to project the solved contact points onto plane P to give the plane points that construct the axial profile of the wheel (see Fig. 4):

$$\begin{cases} z_p(u, \beta, \phi_1) = z_t(u, \beta, \phi_1) \\ y_p(u, \beta, \phi_1) = \sqrt{x_t^2(u, \beta, \phi_1) + y_t^2(u, \beta, \phi_1)} \end{cases} \quad (6)$$

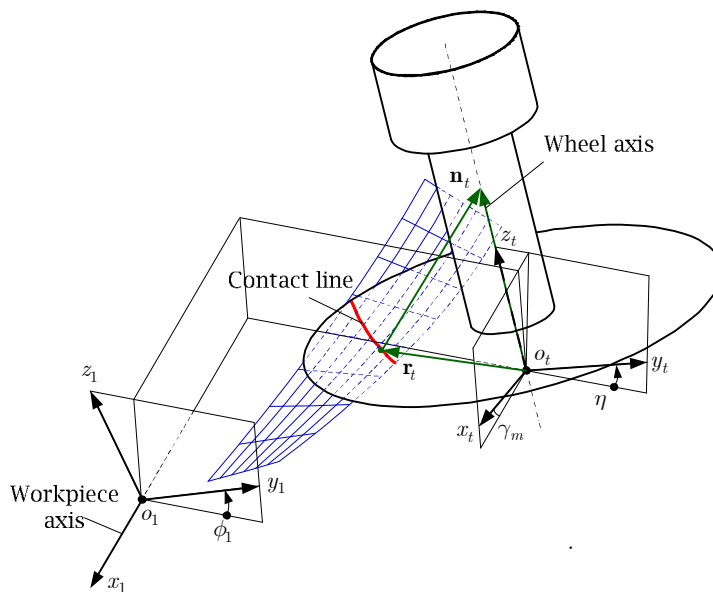


Fig. 3: Conjugate condition between the work-piece and the wheel during the hob sharpening process.

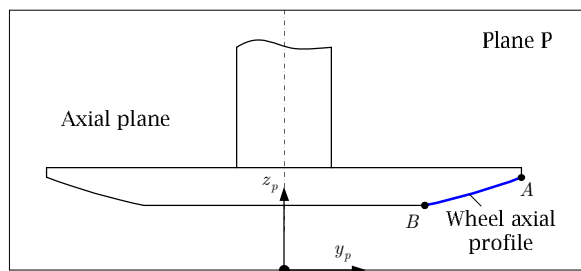


Fig. 4: Axial profile of the wheel for the hob sharpening process.

3 MATHEMATICAL MODEL OF THE FIVE-AXIS CNC HOB SHARPENING MACHINE

The DOF of the proposed Cartesian-type hob sharpening machine is arranged based on the universal CNC hob sharpening grinder, which has five numerically closed-loop controlled axes for grinding and one manual axis for the wheel tilt: three rectilinear motions (C_x, C_y, C_z), two rotational motions (ψ_a, ψ_b), and one manually set angle ψ_c (see Fig. 5). Such a horizontal machine configuration is a common structural design in existing hob sharpening machines. Its coordinate systems $S_t(x_t, y_t, z_t)$ and $S_1(x_1, y_1, z_1)$, whose relative positions are described by the auxiliary coordinate systems from S_d to S_g , are rigidly connected to the grinding wheel and workpiece, respectively. Here, ψ_a is the rotation angle of the workpiece, and ψ_b denotes the swivel angle of the grinding wheel. The horizontal stroke motion C_x and the wheel axial motion C_z are used for the workpiece and the wheel positioning, respectively, while C_y is the radial motion for infeeding the wheel down to tooth depth. The setting angle ψ_c (about 15deg) is used for the wheel tilt, which inclines the wheel to avoid interference between the wheel and the workpiece. Parameters K_1 and K_2 are machine constants that depend on the individual machine and are calibrated immediately after machine installation.

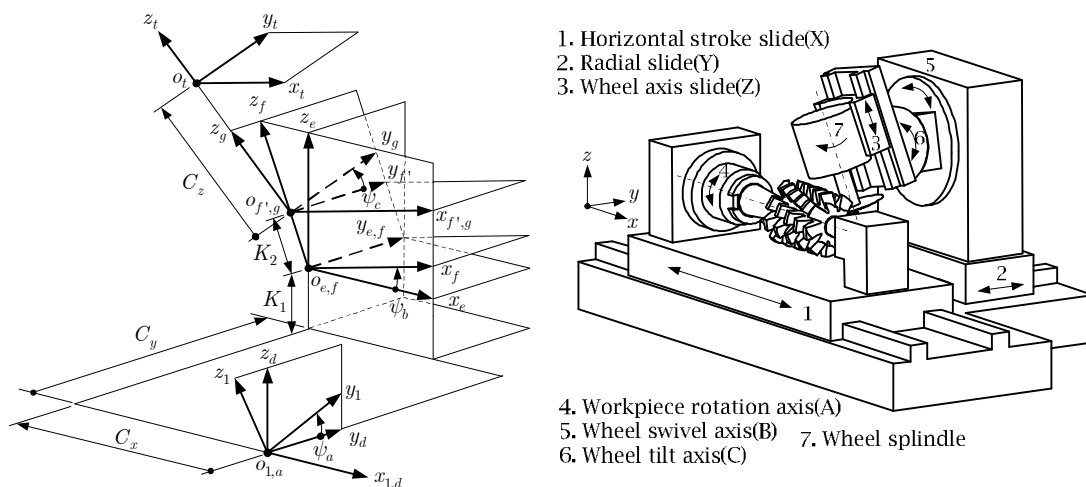


Fig. 5: Coordinate systems of the five-axis CNC hob sharpening machine.

Assuming that, as shown in Fig. 5, the surface position of the wheel is represented in coordinate system S_t in two-parametric form $\mathbf{r}_t(u, \beta)$, which is determined by the solved wheel axial profile (Sect. 2), the transformation matrices S_t to S_1 yield the following surface locus for the wheel represented in coordinate system S_1 :

$$\begin{aligned} \mathbf{r}_1^{(C)}(u, \beta; C_x, C_y, C_z, \psi_a, \psi_b, \psi_c) &= \mathbf{M}_{1d}^{(C)}(\psi_a) \mathbf{M}_{de}^{(C)}(C_x, C_y) \mathbf{M}_{ef}^{(C)}(\psi_b) \mathbf{M}_{fg}^{(C)}(\psi_c) \mathbf{M}_{gt}^{(C)}(C_z) \mathbf{r}_t(u, \beta) \\ &= \mathbf{M}_{1t}^{(C)}(C_x, C_y, C_z, \psi_a, \psi_b, \psi_c) \mathbf{r}_t(u, \beta) \end{aligned} \quad (7)$$

where

$$\begin{aligned} \mathbf{M}_{1d}^{(C)}(\psi_b) &= \begin{bmatrix} 1 & 0 & 0 & 0 \\ 0 & \cos \psi_b & \sin \psi_b & 0 \\ 0 & -\sin \psi_b & \cos \psi_b & 0 \\ 0 & 0 & 0 & 1 \end{bmatrix}, \quad \mathbf{M}_{de}^{(C)}(C_x, C_y) = \begin{bmatrix} 1 & 0 & 0 & -C_x \\ 0 & 1 & 0 & C_y \\ 0 & 0 & 1 & K_1 \\ 0 & 0 & 0 & 1 \end{bmatrix}, \quad \mathbf{M}_{ef}^{(C)}(\psi_b) = \begin{bmatrix} \cos \psi_b & 0 & -\sin \psi_b & 0 \\ 0 & 1 & 0 & 0 \\ \sin \psi_b & 0 & \cos \psi_b & 0 \\ 0 & 0 & 0 & 1 \end{bmatrix}, \\ \mathbf{M}_{fg}^{(C)}(\psi_c) &= \begin{bmatrix} 1 & 0 & 0 & 0 \\ 0 & \cos \psi_c & -\sin \psi_c & 0 \\ 0 & \sin \psi_c & \cos \psi_c & K_2 \\ 0 & 0 & 0 & 1 \end{bmatrix}, \quad \text{and} \quad \mathbf{M}_{gt}^{(C)}(C_z) = \begin{bmatrix} 1 & 0 & 0 & 0 \\ 0 & 1 & 0 & 0 \\ 0 & 0 & 1 & C_z \\ 0 & 0 & 0 & 1 \end{bmatrix}. \end{aligned}$$

The spatial position of the wheel axis relative to the workpiece axis should be the same whether the workpiece is ground on a universal or a CNC machine. Therefore, comparing Eqn. (7) with Eqn. (1) satisfies the following relation:

$$\mathbf{M}_{1t}^{(C)}(C_x, C_y, C_z, \psi_a, \psi_b, \psi_c) = \mathbf{M}_{1t}(\eta, \gamma_m, E_t, L_t, \phi_1) = \mathbf{M}_{t1}^{-1}(\eta, \gamma_m, E_t, L_t, \phi_1) \quad (8)$$

Assuming that the position of the workpiece on the universal hob sharpening machine is the same as on the CNC machine, the angle and translational positions of the CNC machine can be derived as follows through comparison with the rotational and translational matrices in Eqn. (8):

$$\begin{cases} \psi_a(\phi_1) = \phi_1 \\ \psi_b(\phi_1) = \gamma_m \\ \psi_c = \eta \end{cases} \quad \text{and} \quad \begin{cases} C_x(\phi_1) = L_t + K_1 \tan \gamma_m \\ C_y(\phi_1) = E_t - (K_1 \sec \gamma_m + K_2) \tan \eta \\ C_z(\phi_1) = -\sec \eta \sec \gamma_m (K_1 + K_2 \cos \gamma_m) \end{cases} \quad (9)$$

where the universal machine settings include η , γ_m , E_t and L_t . Although all parameters are generally constant, in simulating the auxiliary flank modification (AFM) motion to reduce the actual errors of the hob tooth face, the above movements, except for manual axis ψ_c can be functions of the workpiece rotation angle ϕ_1 (or the position along the hob axis in the case of straight gashes).

The surface locus of the wheel shown above could therefore be generalized in three-parametric form as $\mathbf{r}_1^{(C)}(u, \beta, \phi_1)$, where u and β are surface coordinates and ϕ_1 is the parameter of motion. According to differential geometry, the unit normal to the surface locus may then be represented in coordinate system S_1 by

$$\mathbf{n}_1^{(C)}(u, \beta, \phi_1) = \frac{\frac{\partial \mathbf{r}_1^{(C)}(u, \beta, \phi_1)}{\partial u} \times \frac{\partial \mathbf{r}_1^{(C)}(u, \beta, \phi_1)}{\partial \beta}}{\left| \frac{\partial \mathbf{r}_1^{(C)}(u, \beta, \phi_1)}{\partial u} \times \frac{\partial \mathbf{r}_1^{(C)}(u, \beta, \phi_1)}{\partial \beta} \right|} \quad (10)$$

The surface position and surface normal of the hob tooth face can then be determined using Eqs. (7) to (10) combined with the following equation of meshing and the two boundary equations of the tooth face:

$$f_1^{(C)}(u, \beta, \phi_1) = \mathbf{n}_1^{(C)}(u, \beta, \phi_1) \cdot \mathbf{v}_1^{(t1)}(u, \beta, \phi_1) = \mathbf{n}_1^{(C)}(u, \beta, \phi_1) \cdot \left(\dot{\phi}_1 \frac{\partial \mathbf{r}_1^{(C)}(u, \beta, \phi_1)}{\partial \phi_1} \right) = 0 \quad (11)$$

where $\mathbf{v}_1^{(t1)}$ is the relative velocity between the wheel and the workpiece in coordinate system S_1 .

As is evident, the motions of the five axes are also functions of the workpiece rotation angle and are quite smooth; they can therefore be approximated in terms of the workpiece rotation angle by n -degree Maclaurin polynomials (i.e., Taylor polynomials expanded about $\phi_1=0$):

$$f_i(\phi_1) = f_i(0) + f_i'(0) \cdot \phi_1 + \frac{f_i''(0) \cdot \phi_1^2}{2!} + \dots + \frac{f_i^{(n)}(0) \cdot \phi_1^n}{n!} + R_i^{(n)}(\phi_1) \quad (12)$$

$$\approx a_{i0} + a_{i1}\phi_1 + a_{i2}\phi_1^2 + a_{i3}\phi_1^3 + a_{i4}\phi_1^4 \quad (i = x, y, z, a, b)$$

where i indicates each machine axis and $R_i^{(n)}(\phi_1)$ is the remainder of the Maclaurin series. Because modern sophisticated free-form CNC machines like the Klingelnberg S31-series and the Luren Precision LGH-series machines use polynomials up to the fourth degree, the polynomial coefficients ($a_{i1} \sim a_{i4}$) can be derived directly from Eqn. (9) by solving their derivatives.

4 FLANK CORRECTION FOR THE FIVE-AXIS CNC HOB SHARPENING MACHINE

The tooth faces on the hob gashes need to be ground during hob manufacture or after cutting edge wear. Correct sharpening ensures machined gear accuracy and a longer cutter lifetime. For both straight and helical gash hobs, the tooth face is ground by a modern CNC hob sharpening machine that has five-axis control and sophisticated software for determining the wheel axial profile and automatically generating the dressing and grinding NC codes. Because hob accuracy dominantly influences the quality of the gears produced, hobs are generally evaluated according to DIN 3968 or AGMA 1102-A03 [9] to guarantee hob precision. In practice, the deviations of the ground tooth face are caused by machine error. The existing software only provides a simple correction function to reduce the surface deviations, one that unfortunately is highly dependent on machine operator skill and experience.

To improve the results of flank correction and increase its flexibility, we propose a free-form flank correction method like that used in the manufacture of spiral bevel and hypoid gears, which has become well developed over the last decade. The algorithm of the proposed flank correction method is similar to that developed in Ref. [8]. That is, modulating the design parameters of the tooth face produces a ground surface whose surface topographic point corrections inversely approximate the measured surface topographic errors. Here, the design parameters are the polynomial coefficients ($a_{i1} \sim a_{i4}$) of the five-axis motion functions based on the mathematical model of a CNC hob sharpening machine. This method, which offers a high-order flank correction with fewer limitations than those placed by the virtual universal machine, requires the following steps: (a) calculation of flank coordinates from the five-axis machine settings and the wheel geometry, (b) construction of the sensitivity matrix through small changes in the coefficients of the five-axis motion function based on flank topographic deviation, (c) calculation of the flank topographic errors from simulated flank data or CMM machine measurements, and (d) calculation of the five-axis machine setting corrections to minimize real surface errors using linear regression. Rather than building the sensitivity matrix in the conventional manner by varying the wheel and universal machine settings, we propose a kinematic flank correction method based on the mathematical model of the five-axis hob sharpening machine,

one that modulates only the five nonlinear machine settings. This method produces high-order flank correction through direct simultaneous five-axis control of modern CNC machines.

The ground tooth face can be expressed as a function of parameters (u, β) , which are derived from Eqn. (7) and an additional equation of meshing, Eqn. (11) for the generated surface. Using the polynomial coefficients of the five-axis motion as variables, the tooth surface may be represented as

$$\mathbf{R}_g = \mathbf{R}_g(u, \beta, \zeta_j) \quad (j = 1, \dots, q) \quad (13)$$

where ζ_j indicates the polynomial coefficients and q is their number. According to differential geometry, the surface variation vector is as follows:

$$\delta \mathbf{R}_g = \frac{\partial \mathbf{R}_g(u, \beta, \zeta_j)}{\partial u} \delta u + \frac{\partial \mathbf{R}_g(u, \beta, \zeta_j)}{\partial \beta} \delta \beta + \sum_{j=1}^q \frac{\partial \mathbf{R}_g(u, \beta, \zeta_j)}{\partial \zeta_j} \delta \zeta_j \quad (14)$$

Because vectors $\frac{\partial \mathbf{R}_g}{\partial u}$ and $\frac{\partial \mathbf{R}_g}{\partial \beta}$ are both perpendicular to the surface normal \mathbf{n}_g , taking the inner product of both sides of the above equation with the surface normal gives the following simplified normal surface variation:

$$\begin{aligned} \delta \mathbf{R}_g \cdot \mathbf{n}_g &= \left(\frac{\partial \mathbf{R}_g}{\partial u} \delta u + \frac{\partial \mathbf{R}_g}{\partial \beta} \delta \beta + \sum_{j=1}^q \frac{\partial \mathbf{R}_g}{\partial \zeta_j} \delta \zeta_j \right) \cdot \mathbf{n}_g \\ &= \sum_{j=1}^q \left(\frac{\partial \mathbf{R}_g \cdot \mathbf{n}_g}{\partial \zeta_j} \right) \delta \zeta_j \end{aligned} \quad (15)$$

The normal surface variations at the topographical grid points may then be written in matrix form:

$$\begin{aligned} \begin{Bmatrix} \delta R_1 \\ \vdots \\ \delta R_p \end{Bmatrix} &= \begin{bmatrix} \frac{\partial R_1}{\partial \zeta_1} & \dots & \dots & \frac{\partial R_1}{\partial \zeta_q} \\ \vdots & \ddots & & \vdots \\ \frac{\partial R_p}{\partial \zeta_1} & \dots & \dots & \frac{\partial R_p}{\partial \zeta_q} \end{bmatrix} \begin{Bmatrix} \delta \zeta_1 \\ \vdots \\ \delta \zeta_q \end{Bmatrix} \\ \{\delta R_i\} &= [S_{ij}] \{\delta \zeta_j\} \quad (i = 1, \dots, p; \text{ and } j = 1, \dots, q) \end{aligned} \quad (16)$$

where $\{\delta R_i\}$ represents the normal surface errors of the $p-1$ grid points and 1 circular flank thickness error at the mean point of tooth surfaces, $[S_{ij}]$ is the sensitivity matrix for the polynomial coefficients, and $\{\delta \zeta_j\}$ represents the corrections to the polynomial coefficients. Because the number of polynomial coefficients q is smaller than the number p , however, Eqn. (16) is overdetermined. The corrections can be approximated using a linear regression technique like the least squares method:

$$\{\delta \zeta_j\} = ([S_{ij}]^T [S_{ij}])^{-1} [S_{ij}]^T \{\delta R_i\} \quad (17)$$

Because the sensitivity matrix is ill conditioned and in most cases nearly singular, we calculate the corrections to the polynomial coefficient using singular value decomposition (SVD) to avoid numerical divergence.

5 NUMERICAL EXAMPLES AND DISCUSSION

We illustrate our proposed method using a helical gash hob as the ground workpiece. The main parameters for the hob in the sharpening process - including the hob geometry, the wheel data, the

universal machine settings determined, and the assumed machine constants for a five-axis CNC machine – are listed in Tab. 1. Based on the given hob data, the tooth face of the hob gash $\mathbf{r}_1(u, \beta)$ can be determined using Eqns. (1) and (2). Substituting the universal machine settings into Eqn. (3) gives the surface locus of the ground surface $\mathbf{r}_i(u, \beta, \phi_1)$, and its normal $\mathbf{n}_i(u, \beta, \phi_1)$ can be obtained by Eqn. (4). Because the axis of wheel \mathbf{z}_i is a vector $(0, 0, 1)$, we can use Eqn. (5) to obtain the equation of meshing. Additionally, because the contact lines between the workpiece and the wheel are identical at every instant in the sharpening process, by setting the workpiece rotation angle at $\phi_1 = 0$, and using Eqn. (5) plus one boundary equation of the wheel, we can solve the contact points that will construct the wheel's axial profile (z_p, y_p) using Eqn. (6) as shown in Fig. 4.

This numerical example applies the proposed flank correction method to reduce flank errors during the hob sharpening process. Unlike a conventional machine, however, the modern CNC hob sharpening machine can provide a five-axis interpolation that enables topographic flank correction. Therefore, our illustrative example is based on a virtual Cartesian-type CNC hob sharpening grinder. Based on the determined universal machine settings (η , γ_m , E_t and L_t), and assuming that the machine constants K_1 and K_2 are equal to 100 mm and 10 mm, respectively, the original polynomial coefficients of the five-axis movement and one setting axis for the universal CNC hob sharpening grinder can be derived from Eqn. (9). These results are listed in Tab. 2 (left section), in which the unit of the workpiece rotation angle ϕ_1 is the radian.

Subsequently, based on a sensitivity analysis, the influences of all polynomial coefficients of the five axes on the tooth faces can be separately investigated up to four degrees, although in Fig. 6 we only show the flank sensitivity topographies of the zero-degree coefficient. As Fig. 6 illustrates, in the zero-degree coefficient, all axes greatly influence tooth face thickness, especially axes Z (the wheel axial motion) and A (the workpiece rotation angle). However, although the change in axes Y (the grinding depth), Z (the wheel axial motion), and B (the wheel swivel angle) causes a pressure angle difference, the change in axes X (the horizontal stroke motion) and A has no influence on flank geography, which remains unaffected by the initial positions for the helical motion. Moreover, although all the other coefficients (i.e. except the zero degree) induce a first-degree or above deviation of flank geometry in the lead direction – by the greater sensitivity of the Z and A axes – they have little influence on tooth face thickness. Our analysis therefore suggests that modulating CNC machine axes can reduce the tooth flank deviations caused by machine errors. Nonetheless, this method has limited ability to eliminate second-degree or above errors in the radial direction of the hob. In such a case, although not detailed here, the axial profile of the wheel can be corrected instead.

Items			Values
(A) Hob data			
Normal module	m_n	mm	7.000
Normal pressure angle	α_n	deg	20.000
Outer diameter	d_a	mm	80.000
Pitch diameter	d_p	mm	62.500
Rake angle	γ_c	deg	0
Tooth depth	h	–	21.000
Flute helix angle	β_c	deg	12.626 R.H.
Flute lead	L_c	mm	876.560
Length	l_c	–	140.000

Items			Values
(B) Wheel data			
Outer diameter	d_w	mm	100.000
(C) Universal machine settings			
Tilt angle of the wheel	η	deg	15.000
Setting angle of the wheel	γ_m	deg	12.626
Center distance	E_t	mm	69.446
Axial movement	L_t	mm	$139.509\phi_1$
(D) Assumed machine constants			
Distance b/w O_d and O_e along z_e	K_1	mm	100.000
Distance b/w O_g and O_f along z_f	K_2	mm	10.000

Tab. 1: Basic parameters for hob sharpening in the numerical example.

Machine axes		Uncorrected hob gash	Corrected hob gash
$C_x = f_x(\phi_1)$	mm	$22.4 + 139.509\phi_1$	$22.4001 + 139.5090\phi_1 + 3.0132E-06\phi_1^2 - 7.1284E-09\phi_1^3 - 1.3495E-06\phi_1^4$
$C_y = f_y(\phi_1)$	mm	39.3078	$39.2943 - 0.0003\phi_1 + 0.0009\phi_1^2 - 0.0001\phi_1^3 - 0.0001\phi_1^4$
$C_z = f_z(\phi_1)$	mm	-116.446	$-116.8590 + 0.0039\phi_1 - 0.0233\phi_1^2 - 3.3273E-5\phi_1^3 - 0.0030\phi_1^4$
$\psi_a = f_a(\phi_1)$	rad	ϕ_1	$-0.0141 + 1.0036\phi_1 - 0.0008\phi_1^2 - 4.4503E-07\phi_1^3 - 2.0862E-05\phi_1^4$
$\psi_b = f_b(\phi_1)$	rad	0.2203	$0.2364 + 0.0004\phi_1 - 0.0024\phi_1^2 + 0.0001\phi_1^3 - 0.0003\phi_1^4$

Tab. 2: Uncorrected and corrected kinematic positions of the CNC hob sharpening machine's five-axis machine axes.

The actual flank topographic errors of the hob gash's tooth face made by the sharpening process can be measured using a gear measurement tool like the Klingelnberg P-series machine. In this example, the flank topographic errors $\{\delta R_i\}$ are assumed to be as given in Fig. 7(a). The sum of squared errors (topographic points) and the maximum thickness error are $576,635\mu m^2$ and $+1.5\mu m$, respectively, so they can be reduced by modulation of the five-axis CNC movement. Substituting the given flank topographic errors $\{\delta R_i\}$ and the sensitivity matrix $[S_{ij}]$ into Eqn. (17) allows calculation of the corrections $\{\delta\zeta_j\}$ to the polynomial coefficients. Adding the corrections into the original polynomial coefficients of the five-axis movement (Tab. 2, left section) then yields the corrected polynomial coefficients, which are listed in the right section of Tab. 2. Figure 7(b) shows the simulated flank topographic errors after a one-time correction for hob sharpening. As the figure illustrates, the proposed correction method can efficiently reduce flank errors. The sum of squared errors and the maximum thickness error are reduced to $37.9\mu m^2$ and

$0\mu m$, respectively. Because compensation of the A axis position only corrects tooth thickness, thickness error can be eliminated completely.

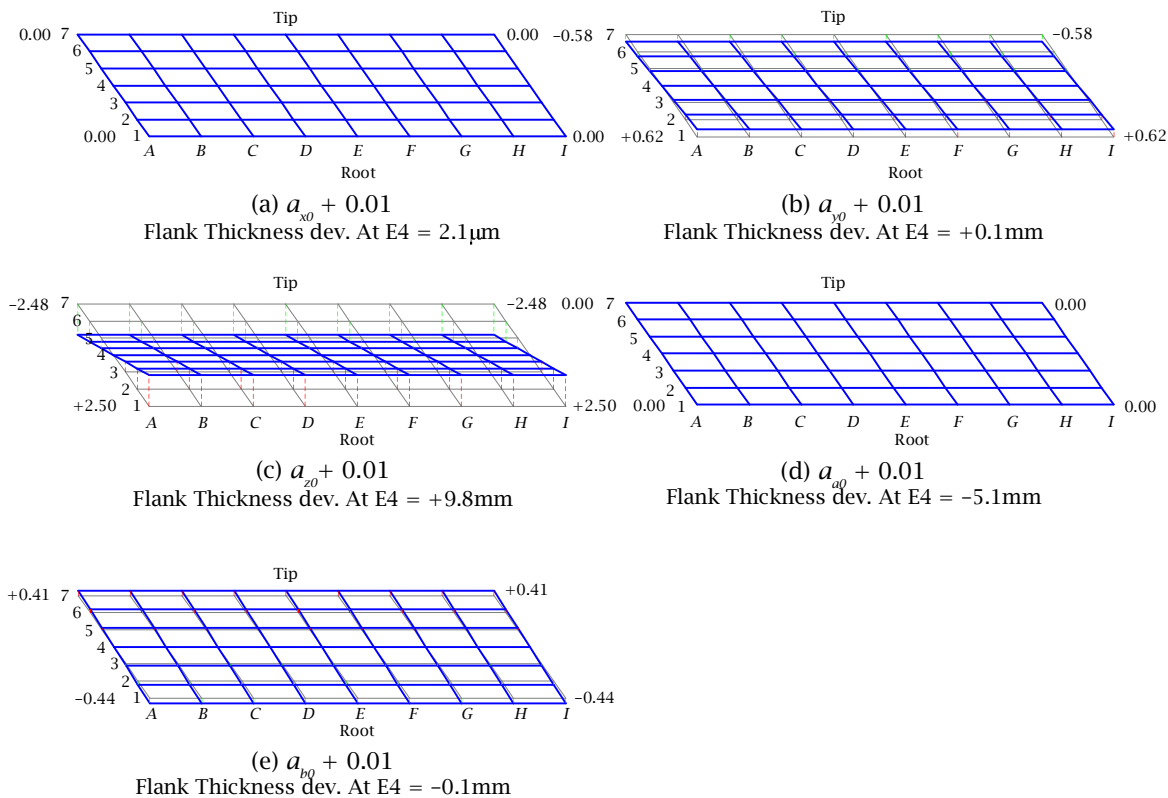


Fig. 6: Flank sensitivity topographies corresponding to the zero-degree polynomial coefficients for the five-axis movement.

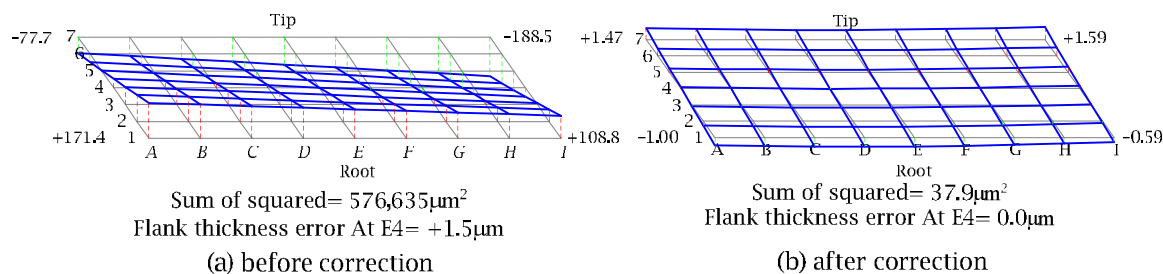


Fig. 7. Simulated flank topographic errors of the five-axis hob sharpening machine during hob sharpening.

6 CONCLUSIONS

This paper has established a mathematical model of the five-axis CNC hob sharpening grinding machine, which is comparable to the Klingelnberg S31-series and the Luren Precision LGH-series machines. In this model, the five-axis machine settings are formulated up to the fourth degree as

functions of Maclaurin polynomials that can be converted from the universal machine settings. This mathematical model of a five-axis machine enables successful grinding of both straight and helical gash hobs.

Based on the proposed mathematical model, we also developed a kinematic flank correction method, which is validated by one numerical example using the helical gash hob. To provide more accurate flank correction, we also built a sensitivity matrix for the model using a topographical deviation that corresponds to the polynomial coefficients of a five-axis movement. Subsequently, using a linear regression technique, we calculated the corrections of the polynomial coefficients based on the corresponding flank errors and sensitivity matrix, although such corrections could also be calculated using optimization techniques and a nonlinear least-squares approach. Here, the proposed flank-correction methodology is derived directly from the five-axis grinding machine, in which high-order correction is easily achievable through direct control of the CNC axis motion. The modern hob sharpening machine is also sufficiently accurate for all axes to be defined by a Maclaurin polynomial up to the fourth degree and is safe for a polynomial up to the sixth order.

One additional advantage of the proposed sensitivity approach is that the flank sensitivity topographies evaluated provide the user with valuable information about the grinding machine axes. Most particularly, these topographies illustrate the precision demand of the machine axes, showing, for example, that the Z and A axes are more sensitive than the other axes and in practice need more precision. Nonetheless, because modulating the machine axes cannot eliminate second-degree or above errors in the radial direction of the hob, further investigation is needed into the correction of the wheel surface.

7 ACKNOWLEDGEMENTS

The authors are grateful to the National Science Council of the R.O.C for its financial support. Part of this work was performed under Contract No NSC 99-2622-E-194-007-CC2.

8 REFERENCES

- [1] Yoshino, H.; Ikeno K.: Error Compensation for Form Grinding of Gears, Transactions of the Japan Society of Mechanical Engineers Part C 57 (543), 1991, 3652-3655.
- [2] Nishida N.; Kobayashi Y.; Ougiya Y.; Tsukamoto N.: Profile Calculation Method for Form Grinding Wheels (1st report). Grinding Wheels for Helical Gears and Avoidance of Interferences, Journal of the Japan Society for Precision Engineering 58 (4), 1992, 628-634.
- [3] Kobayashi Y.; Nishida N.; Ougiya Y.; Nagata H.: Tooth Trace Modification Processing of Helix Gear by Form Grinding Method, Transactions of the Japan Society of Mechanical Engineers Part C 61 (590), 1995, 4088-4093.
- [4] Kobayashi, Y.; Nishida, N.; Ougiya, Y.; Nagata, H.: Estimation of Grinding Wheel Setting Error in Helical Gear Processing by Form Grinding, Transactions of the Japan Society of Mechanical Engineers Part C 63(612), 1997, 2852-2858.
- [5] Chang, S.-L.: Precision Grinding of Helical Gashes for Hob Cutters, Journal of the Chinese Society of Engineers, 23(4), 2002, 313-320.
- [6] Chang, S.-L.: Helix Gash of Hob Cutter Manufactured by Milling Cutter, Journal of Material Processing Technology, 142(2), 2003, 569-575. DOI: 10.1016/S0924-0136(03)00661-7
- [7] Litvin, F. L.; Fuentes, A.: Gear Geometry and Applied Theory, second ed., Cambridge University Press, New York, NY, 2004. DOI: 10.1017/CBO9780511547126

- [8] Shih, Y.-P.; Fong, Z.-H.: Flank Correction for Spiral Bevel and Hypoid Gears on a Six-Axis CNC Hypoid Gear Generator, ASME Journal of Mechanical Design, 130(6), 2008, 062604. DOI: 10.1115/1.2890112
- [9] ANSI/AGMA1102-A03, Tolerance Specification for Gear Hobs, Alexandria, VA, 2008.